Transcriptomics analyses of the LRRK2 protein interactome reveal distinct molecular signatures for sporadic and LRRK2 Parkinson's Disease

Yibo Zhao[1], Kirsten Harvey[1], Valentina Escott-Price[2], Patrick A Lewis[3,4], Claudia Manzoni[1*]

1. UCL School of Pharmacy, dept Pharmacology, London, United Kingdom.

2. University of Cardiff, School of Medicine, Division of Psychological Medicine and Clinical Neurosciences, Cardiff, United Kingdom

3. Royal Veterinary College, London, United Kingdom.

4. UCL Queen Square Institute of Neurology, London, United Kingdom.

* Corresponding: c.manzoni@ucl.ac.uk

Abstract:

Mutations in the *LRRK2* gene are an important genetic cause for familial Parkinson's Disease (LRRK2-PD) and clinical trials are ongoing to evaluate the benefits associated with the therapeutical reduction of LRRK2 kinase activity. In this study, we aimed at modelling the molecular milieu surrounding LRRK2 and describe the changes that occur during disease with the aim of contrasting and comparing sporadic PD and LRRK2-PD. We analysed the molecular expression profiles (whole blood mRNA) of LRRK2's protein interactors in the sporadic vs familial PD conditions and found interesting differences between the 2 scenarios. Our results showed that LRRK2 interactors not only presented different alterations in expression levels in sporadic and familial PD while compared to controls; they also exhibited distinct co-expression behaviours in the 2 PD conditions. These results suggest that, albeit being classified as the same disease based on clinical features, LRRK2-PD and sporadic PD show significant differences from a molecular perspective.

Introduction

Leucine-rich repeat kinase 2 is a large (over 250 kDa), multifunctional enzyme encoded by the *LRRK2* gene, possessing 2 enzymatic (GTPase and Kinase) and 4 scaffold (Armadillo, Ankyrin, LRR and WD40 motifs) domains (Berwick et al., 2019). LRRK2 is able to interact with a vast number of protein partners (Zhao et al., 2023) and is involved in a large number of biological processes such as vesicular transport, autophagy, regulation of cellular response to stress, regulation of cell cycle, etc (Albanese et al., 2019; Chen et al., 2017; Hsu et al., 2010; Sanna et al., 2012). Mutations in LRRK2 are an important genetic cause of familial PD (fPD) overall with 1 to 40% of fPD cases associated with LRRK2 depending on the population under study (Bras et al., 2005; Greggio et al., 2008; Lesage et al., 2006; Ozelius et al., 2006). Since 2004, when a missense change on the *LRRK2* gene was firstly associated with fPD, numerous coding and non-coding variants of LRRK2 have been identified in PD families, among which the G2019S and R1441C/G mutations are the 2 most common pathogenic variants occurring on the kinase and GTPase domains of the LRRK2 protein respectively (Dauer & Ho, 2010; Esteves et al., 2014; Giesert et al., 2017; Henry et al., 2015; Paisán-Ruiz et al., 2013). However, how these pathogenic changes contribute to fPD is still unclear. Additionally, polymorphisms, mainly in the promoter of *LRRK2*, have

been linked to sporadic PD (sPD) (Nalls et al., 2019) and upregulated LRRK2 kinase activity has also been related with sPD. For example, PD-related inflammation both in the Central Nervous System (CNS) and at the periphery, was linked to an increased LRRK2 expression level and strengthened LRRK2 kinase activity in microglia and peripheral immune cells in sPD patients as compared to controls (Cook et al., 2017; Di Maio et al., 2018). All the above-mentioned findings indicate that LRRK2 is crucial for the understanding of PD etiopathogenesis, additionally LRRK2 might constitute a link between familial and sporadic forms of the disease.

However, from a clinical perspective, LRRK2-PD and sPD have been reported with some distinct features. Despite having similar motor-symptoms (such as bradykinesia, tremor, rigidity, and postural instability) as well as sharing some of the non-motor symptoms (Haugarvoll et al., 2008; Healy et al., 2008; Kluss et al., 2019), patients with LRRK2-PD show slower decline considering both movement and cognitive impairment (Alcalay et al., 2015; Srivatsal et al., 2015). In addition, LRRK2-PD and sPD show slightly different pathological features. For example, LRRK2-PD patients exhibit less α-synuclein aggregation in Cerebrospinal Fluid (CSF), feature that is a hallmark of sPD (Garrido et al., 2019; Rivero-Ríos et al., 2020) as well as increased basal forebrain volume, which is probably as a compensation in the cholinergic system (Batzu et al., 2023). Such differences might highlight an intrinsic variation at the molecular level between these 2 forms of PD thus suggesting different model systems might be required to investigate them. Also, this consideration may pose a problem in translational research, for example the use of LRRK2 inhibitors in clinical trials (Tolosa et al., 2020) might require patient stratification.

In this study we hypothesized that despite being generally regarded as the same disease, sPD and LRRK2-PD might have a different molecular signature and therefore the molecular alterations contributing to disease onset and progression might be functionally different. We constructed the protein-protein interaction (PPI) network around *LRRK2* ($LRRK2_{net}$) and evaluated the expression changes within the $LRRK2_{net}$ (absolute level of expression as well as co-expression) in a cohort of sPD and LRRK2-PD patients in comparison with healthy controls. The results provide a bioinformatic proof that the signature of expression changes in the $LRRK2_{net}$ is dissimilar in sPD vs LRRK2-PD showing significant differences in both gene expression and co-expression, suggesting the molecular pathways at the base of these two conditions might be different. This is relevant for the understanding of the different molecular mechanisms of PD and it highlights the necessity for patient stratification in both discovery research and clinical trials, suggesting different therapeutic approaches might be needed if we intend to move from symptomatic to effective disease treatment.

Method

Construction of LRRK2 PPI Network

PPIs (edges) connecting LRRK2 with its direct interactors were defined as "1st-layer" interactions and were downloaded via PINOT v1.1 (http://www.reading.ac.uk/bioinf/PINOT/PINOT_form.html), HIPPIE v2.3 (http://cbdm-01.zdv.uni-mainz.de/~mschaefer/hippie/index.php) and MIST v5.0 (https://fgrtools.hms.harvard.edu/MIST/) (Alanis-Lobato et al., 2017; Hu et al., 2018; Tomkins et al., 2020) on 16th March 2023 and the LRRK2 interactome was built following the pipeline in (Zhao et al., 2023). In summary: to access the most comprehensive set of LRRK2 interactors, "Lenient" filter level was applied in PINOT; while no filter was applied for HIPPIE and MIST to download the entire set of raw interaction to be filtered in a second step. Interactors retrieved from the 3 tools were merged and quality-controlled to identify interactors with missing publication identifier, missing interaction

detection method, no conversion to a standard gene identifier, and with low interaction confidence score. The "2nd-layer" interactions were identified as PPIs (edges) among LRRK2 interactors (other than LRRK2 itself) and were downloaded via HIPPIE (v2.3) on 16th March 2023. Of note, only PPIs with high confidence score (≥ 0.72) were kept for further analysis in the 2nd layer. The LRRK2 PPI network ($LRRK2_{net}$) was constructed by combining the "1st-layer" and "2nd-layer" interactions. Centrality measures on the $LRRK2_{net}$ were derived considering the degree of each node and by the Cytoscape measure plug-in.

PPMI Whole blood RNA-Seq data download

Transcript-QC: whole blood mRNA data (read counts) for LRRK2 interactors at baseline (BL = time at diagnosis) were retrieved using Ensembl gene ID from the Parkinson's Progression Marker Initiative (PPMI) dataset on 24th January 2023. PPMI – a public-private partnership – is funded by The Michael J. Fox Foundation for Parkinson's Research and funding partners, including those reported at https://www.ppmi-info.org/about-ppmi/who-we-are/studysponsors. Transcripts of LRRK2 interactors with read counts ≤ 15 in more than 75% samples were removed. Sample-QC: PPMI is an ongoing observational, international, multicenter cohort study aimed at identifying the biomarkers of PD progression in a large cohort of participants (https://www.ppmi-info.org/). PPMI cohorts of "de novo PD" and "healthy control" were included in this study. Subjects from the 2 cohorts were further filtered to keep only those with robust genetic status records using the following criteria: confirmed by at least 3 out of 6 detection techniques (WGS, WES, RNA-Seq, GWAS, CLIA, SANGER) of which 1 should be a next generation sequencing technique (WGS, WES, RNA-Seq) and 1 should be a screening technique (GWAS, CLIA, SANGER). Of note, subjects with mutations in PD genes other than LRRK2 (*GBA*, *PINK*, *Parkin* and *SNCA*) were excluded to avoid potential bias. QC-ed subjects were allocated into 3 cohorts: Control, Sporadic PD (sPD, with no *LRRK2* or other gene mutations in record) and LRRK2-PD (only with *LRRK2* mutations considered to be pathogenetic – i.e., G2019S, R1441C/G). Read counts retrieved from PPMI were extracted for the 3 cohorts, thereby forming the "PPMI_Matrix".

Differential Expression Analysis (DEA) and Co-expression analysis (CEA)

The "PPMI_Matrix" was QC-ed using the R package "WGCNA" (function: "goodSampleGenes") (Langfelder & Horvath, 2008). The PPMI_Matrix was utilised to perform DEA to compare the expression levels of LRRK2 interactors in the control, sPD and LRRK2-PD cohorts using the R package "DESeq2" and calculating fold change (FC) for each of the LRRK2 interactors (i) in [sPD vs control] and [LRRK2-PD vs control]. Data normalisation and p-value adjustment for multiple comparisons were performed automatically by "DESeq2". Of note, results from DEA were adjusted for sex. LRRK2 interactors were considered up(down) regulated when log2FC > 0 (log2FC < 0) and adjusted-p < 0.05 in [sPD vs control] or [LRRK2-PD vs control]. Upregulated interactors received a score of 1 and downregulated interactors received a score of -1. Interactors whose expression level was not changed in comparison with controls received a score = 0.

Weighted Gene Co-expression Network Analyses (WGCNA) were performed on the PPMI_Matrix to identify co-expression modules within the $LRRK2_{net}$ for the sPD and LRRK2-PD cohorts (hereby referred as "M_sPD" and "M_LPD"). The modules in M_sPD and M_LPD were compared in terms of their composition of LRRK2 interactors to identify conservation across the cohorts. For every 2 co-expression modules, the number of overlapping proteins (test_overlap) was compared to the overlap count distribution generated by 1000 pairs of randomly sampled protein lists from the $LRRK2_{net}$ (random_overlap). A significant overlap between 2 modules was defined as: 1) test_overlap > 95% of the points in the random overlap distribution curve and 2) the percentage of overlapped interactors

(Overlap Rate) in both of the 2 modules > 60%. The random_overlap distribution curve was considered as normally distributed.

Weighted Network Analysis

Topological clusters in the $LRRK2_{net}$ were extracted using the Fast Greedy Clustering algorithm (after removing: i) LRRK2 itself, ii) nodes with degree of 1, and iii) triangle motifs) on the basis of edge betweenness. Topological clustering and network visualisation was performed using Cytoscape (Shannon et al., 2003b). The edges in each of the obtained topological cluster were classified in up/downregulated edges based on the following criteria: A) upregulated edge= i) at least 1 of the 2 nodes connected by the edge had increased expression level in sPD and/or LRRK2-PD vs controls or ii) a strong positive co-expression (Pearson's coefficient > 0.6) was observed for the 2 nodes connected via the edge in sPD and/or LRRK2-PD but not in controls; B) downregulated edge= i) at least 1 of the 2 nodes connected by the edge presented decreased expression level in sPD and/or LRRK2-PD vs controls or ii) a strong positive co-expression (Pearson's coefficient > 0.6) for the 2 nodes connected via the edge was observed in the controls but not in sPD and/or LRRK2-PD cases. The percentage of upregulated, downregulated and unchanged edges for each single topological cluster were calculated for the sPD and the LRRK2-PD scenarios and compared via One Sample Proportion Test to identify the trend of each topological cluster and qualitatively define whether a cluster was mainly up/down regulated or unchanged in sPD or LRRK2-PD vs controls.

Finally, to better quantify the alteration of cluster A in sPD vs LRRK2-PD, each edge was weighted ($S_{(i,j)}$) using the following: $S_{(i,j)} = S_{Coex(i,j)} + 0.5 \times S_{DEA(i)} + 0.5 \times S_{DEA(j)}$, in which $S_{Coex(i,j)}$ represents the co-expression score between genes *i* and *j* (if Pearson's Coefficient > 0.6, $S_{Coex(i,j)} = 1$; otherwise $S_{Coex(i,j)} = 0$); $S_{DEA(i)}$ and $S_{DEA(j)}$ represent the DEA score of interactor *i* and *j* in the sPD or LRRK2-PD cohorts vs controls. Of note, the correlation values were binarized in order to make them comparable with the DEA expression values and give both the same weight. Following this definition, edges with $|S_{(i,j)}|$ = 0.5 are mildly affected by PD (up-regulated/down-regulated), i.e., with only one interactor changed in expression level; edges with $|S_{(i,j)}|$ = 1 are moderately affected, i.e., with both of the interactors changed in expression level or a damaged co-expression linkage between the 2 interactors; edges with $|S_{(i,j)}|$ ≥ 1.5 are highly affected by the disease condition, i.e., with ≥ 1 interactors changed in expression level and a damaged co-expression linkage.

Functional enrichment analysis

Functional annotation was performed via g:Gost from the g:Profiler toolset (Raudvere et al., 2019) considering Gene Ontology Biological Processes (GO-BP). The number of significantly enriched GO-BP terms (Bonferroni corrected p-value < 0.05) was counted as "Enrichment Score" (ES). Significantly enriched terms were processed via text mining to highlight the re-occurring key words via the R package "Wordcloud". Semantically similar words exacted via text mining were manually combined, e.g., "necrotic", "necroptotic" and "necroptosis" were considered as the same functional word and the frequencies were thereby combined. Additionally, general words were excluded as they are not able to represent the specific functions of the topological cluster, e.g., "of", "in", "biological", "involved", etc. The top 10 words with the highest frequency in functional annotation were defined as "key words" for a given topological cluster, thereby representing the main biological processes sustain by the cluster of LRRK2 interactors.

Software

Data processing was performed in Excel and with R and Python packages. Cytoscape (Shannon et al., 2003a) was used to draw the networks.

Results

$LRRK2_{net}$ Construction

LRRK2 interactors (N = 418, **Table S1**) were downloaded via an in-house pipeline (Zhao et al., 2023) and they constituted the 1st-layer of interactions within the $LRRK2_{net}$ as they all connected to a single node only (i.e., LRRK2). The 2nd-layer of interactions was built by considering the edges linking across all the 418 LRRK2 interactors. To build this 2nd-layer, a total of 4860 PPIs among LRRK2 interactors were extracted via HIPPIE (v2.3), among which 1466 (30.2%) presented high confidence score (≥ 0.72) and were retained (**Table S2**). After removing self-interactions (n = 121), a total number of 1345 QC-ed 2nd-layer PPIs were kept for network construction. By combining the 1st-layer and the 2nd-layer interactions, a PPI network was constructed around LRRK2, which contained 418 nodes and 1762 edges ($LRRK2_{net}$, **Figure 1A**). Centrality analysis showed that the degree distribution of the $LRRK2_{net}$ followed the power law: 84.8% interactors (N = 357) were associated with low degrees (≤ 14); while 9.8% interactors (N = 41) were characterized by moderate degrees (between 15 and 24). Finally, only a total of 21 interactors (5.0%) presented high degrees (≥ 25), thereby forming the denser portion of the $LRRK2_{net}$ (named "backbone", **Figure 1B**). The nodes within the backbone of the $LRRK2_{net}$ were defined as "sub-hub proteins" of the $LRRK2_{net}$ (with LRRK2 being the central hub due to network construction), among which TP53 (degree = 69), CDK2 (degree = 49), HSPA8 (degree = 47), HSP90AB1 (degree = 45), HSP90AA1 (degree = 44), YWHAZ/14-3-3Z (degree = 44), and LAPR7 (degree = 40) presented with the highest degree centrality, suggesting their potential role as central mediators in LRRK2 signalling pathways.

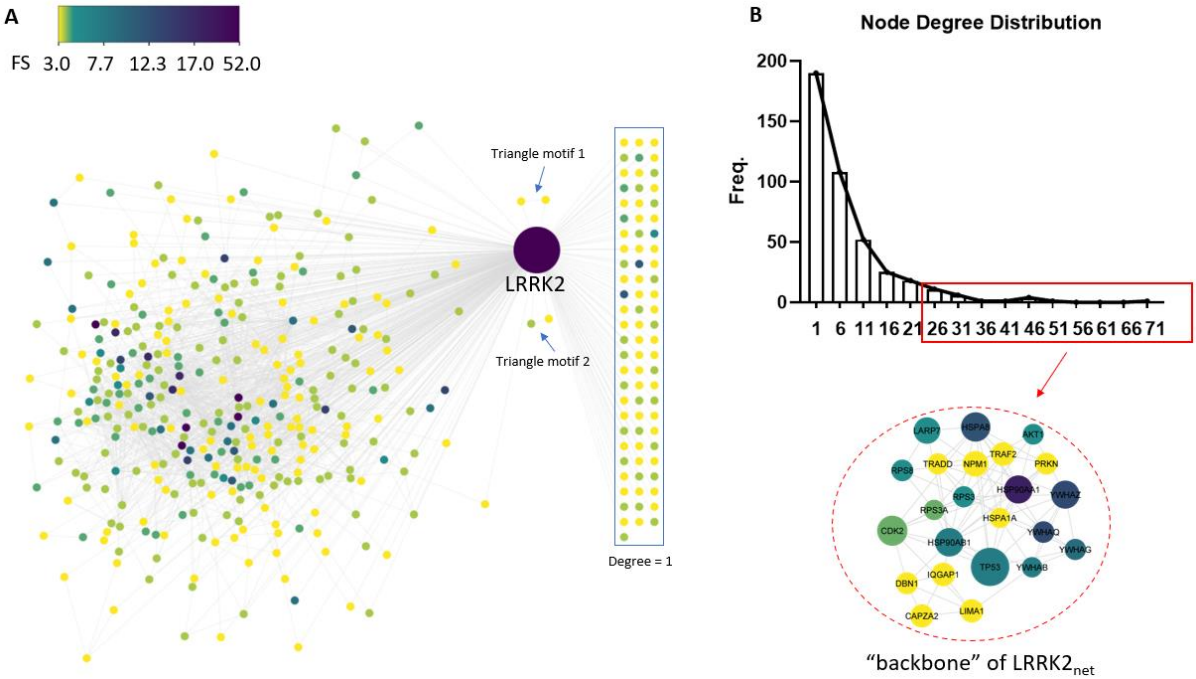

Figure 1. The $LRRK2_{net}$ A) The *$LRRK2_{net}$ contains a total of 418 interactors (represented as nodes) and 1762 PPIs (represented as edges). Interactors were colour-coded based on their Final Scores (FS) calculated from the QC pipeline as the total number of publications + the total number of detection methods with which an interactor was reported in literature. FS is therefore a measure indicating the*

reproducibility of each interactor. The darker the colour, the higher the FS, the larger the amount of evidence in literature for the interactor. Of note, all the 418 interactors have a FS ≥ 3 (i.e., reported at least in > 1 publication or with > 1 detection method). The design of the network highlights the nodes with degree = 1 (nodes to the right side of LRRK2), these nodes connect only with LRRK2 but not with the other nodes in the network. Two triangle motifs were identified in the LRRK2$_{net}$ (marked with blue arrows). A triangle motif includes LRRK2 and 2 other interactors linked with each other but not connected with the rest of the network. ***B)*** *Centrality analysis showed that the degree distribution of the LRRK2$_{net}$ follows the power law: only 21 (5.0%) interactors presented with high degrees (≥ 25) constituting the "backbone" of LRRK2$_{net}$.*

Differential Expression Analysis (DEA) of the LRRK2$_{net}$ in PD cases vs controls

RNA-Seq read counts (rc) were retrieved for 415 (out of 418) LRRK2 interactors and for 657 PPMI subjects (controls = 170; sPD cases = 371; and LRRK2-PD cases = 116). A total of 38 interactors were removed due to low rc. Rc for the remaining 377 interactors formed the PPMI_Matrix. DEA results showed that: the mRNA levels of 64 interactors (17.0%) were significantly altered in the LRRK2-PD condition (in comparison to controls), with 36 down-regulated and 28 up-regulated interactors (adjusted-p < 0.05, **Figure 2A, Table S3**). A total of 53 interactors (14.0%) presented significant changes in expression levels in sPD in comparison with controls, including 29 down-regulated and 24 up-regulated interactors (adjusted-p < 0.05, **Figure 2B**). Down-regulated interactors in the LRRK2-PD condition (N = 36) presented a significantly larger decrease in expression level as compared to the ones down-regulated in the sPD condition (N = 24) (mean log2FC = -0.19 vs. -0.15 respectively; t-test p = 0.031); while no significant difference was observed for up-regulated interactors (**Figure 2C**) meaning that if LRRK2 interactors are downregulated, they are globally more downregulated in LRRK2-PD as compared to sPD. Of note, only a total of 17 interactors presented with the same alteration in LRRK2-PD and sPD, in which 14 interactors were down-regulated while 3 interactors were up-regulated, suggesting these LRRK2 interactors are consistently affected during PD progression regardless of the existence of a *LRRK2* mutation (**Figure 2D**). GO-BP enrichment analysis showed that these 17 interactors were associated with biosynthesis, metabolism and translation processes (**Figure 2E**). Of note, no interactors exhibited opposite trend of differential expression in sPD vs LRRK2-PD (i.e., upregulated vs downregulated).

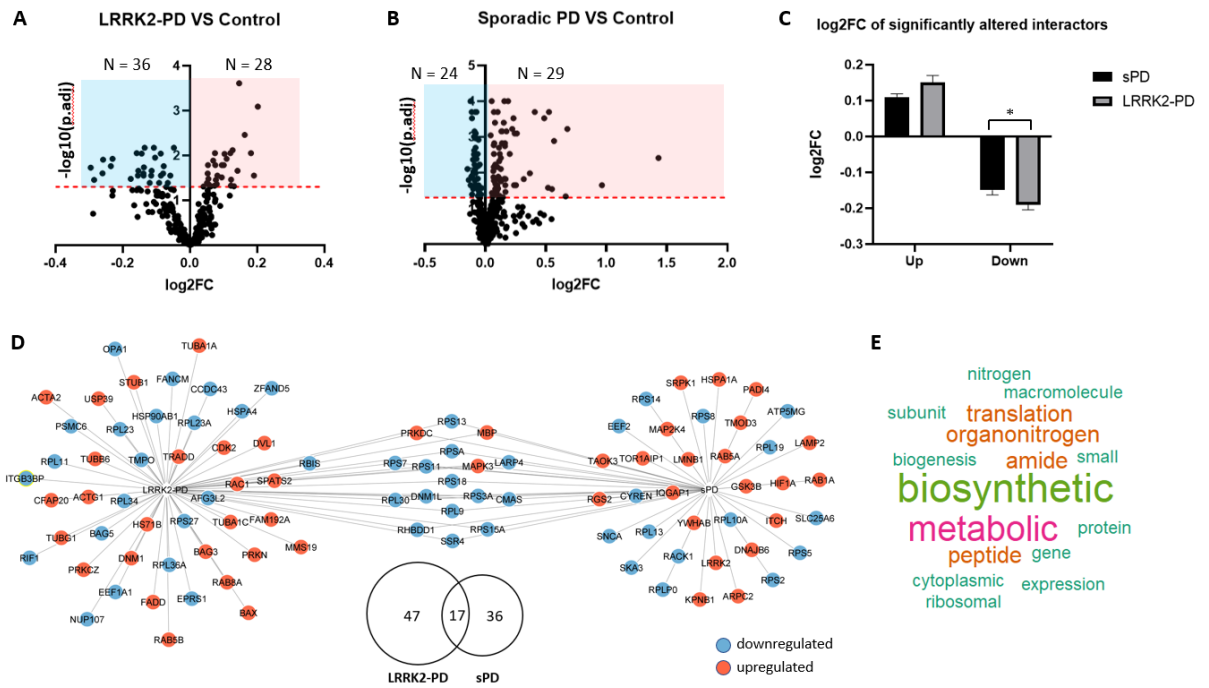

Figure 2. DEA for the LRRK2$_{net}$ ***A)*** *The volcano plot shows DEA results for the 377 LRRK2 interactors whose whole blood RNA expression levels were available comparing the LRRK2-PD cohort vs controls. The X-axis represents log2 Fold Change (log2FC); the Y-axis represents -log10 transformed adjusted-p values. The red horizonal line represents the threshold of adjusted-p = 0.05. LRRK2 interactors in the red area (on the right side) were considered upregulated (N = 28) while those in blue area (on the left side) were considered downregulated (N = 36).* ***B)*** *The volcano plot shows DEA results for LRRK2 interactors comparing the sPD cohort vs controls. LRRK2 interactors in the red area (on the right side) were considered upregulated (N = 29) while those in blue area (on the left side) were considered downregulated (N = 24)* ***C)*** *The bar graph shows the average log2FC for the interactors with significantly down or up-regulated expression levels in sPD and LRRK2-PD; a significantly larger decrease was observed in the LRRK2-PD cohort as compared to the sPD cohort (t-test p = 0.031); while upregulated interactors were affected to the same extent.* ***D)*** *The Venn graph and the network graph show 17 LRRK2 interactors presenting the same differential expression pattern in the LRRK2-PD and the sPD cohorts in comparison with controls. In the network graph, interactors were colour-coded based on upregulation (red) and downregulation (blue). E) The word cloud represents the functional keywords returned by GO-BP enrichment on the 17 interactors that presented same differential expression pattern in the 2 PD conditions. The larger the text is, the higher the frequency the keyword appeared in the enrichment results.*

Co-expression Analysis (CEA) of the LRRK2$_{net}$

WGCNA was performed using the PPMI_Matrix to identify co-expressed modules across the LRRK2 interactors in the 3 conditions under evaluation (i.e sPD, LRRK2-PD and controls). Five co-expression modules were identified in both PD cohorts: M1-5_sPD and M1-5_LPD (**Figure 3A**, **Table S4, Figure S1A,B**). These 10 modules were compared to assess similarity based on node composition. M1_sPD (number of LRRK2 interactors in the module = N = 94) and M1_LPD (N = 95) showed significant overlap ($p < 0.001$), with 69 conserved LRRK2 interactors across the 2 PD cohorts (Overlap Rate = 73.4% and 72.6%, respectively), suggesting that the interactors in these 2 modules have conserved co-expression behaviour in spite of the presence of the *LRRK2* mutation (**Figure 3B, Table S5**). GO-BP enrichment

analysis showed that the conserved M1_sPD and M1_LPD are associated with protein localisation, response to stress and metabolism (**Table S6**). Similarly, M2_sPD (N = 85) and M5_LPD (N = 59) exhibited a significant overlap of 53 interactors (Overlap Rate = 62.4% and 89.8%, respectively; $p < 0.001$) with association with ribosomal functionality based on GO-BPs enrichment analysis (**Figure 3C**, **Table S5, S6**). Of note, 30 out of the 53 shared interactors were ribosomal proteins. In addition, 21 of them presented similar alterations in sPD and LRRK2-PD as identified in DEA. The remaining 3 sPD and 3 LRRK2-PD modules presented certain levels of overlap but none was significant ($p > 0.05$ and/or Overlap Rate < 60%). Of note, the hub protein LRRK2 was contained in the modules M4_LPD (N = 35) and M5_sPD (N = 49), suggesting that the interactors within these specific modules are the ones that are preferentially co-expressed with LRRK2 in the LRRK2-PD and sPD condition, respectively (**Figure 3D**); of note these 2 models are statistically different between the 2 PD conditions. GO-BP enrichment showed that both M4_LPD and M5_sPD were related to organelle organisation, while M5_sPD only was also associated with cell division, cell death, signal transduction and cytoskeleton organisation (**Table S6**).

In summary, even though some module overlaps were identified, the 5 modules isolated via WGCNA in sPD and LRRK2-PD were not composed of the same proteins suggesting that even if some co-expression changes are similar in the 2 PD conditions (2 out of 5 modules do present a significant overlap) there are also a number of co-expression changes in the LRRK2 interactome that are unique to sPD or to LRRK2-PD (3 out of 5 modules are unique to the condition).

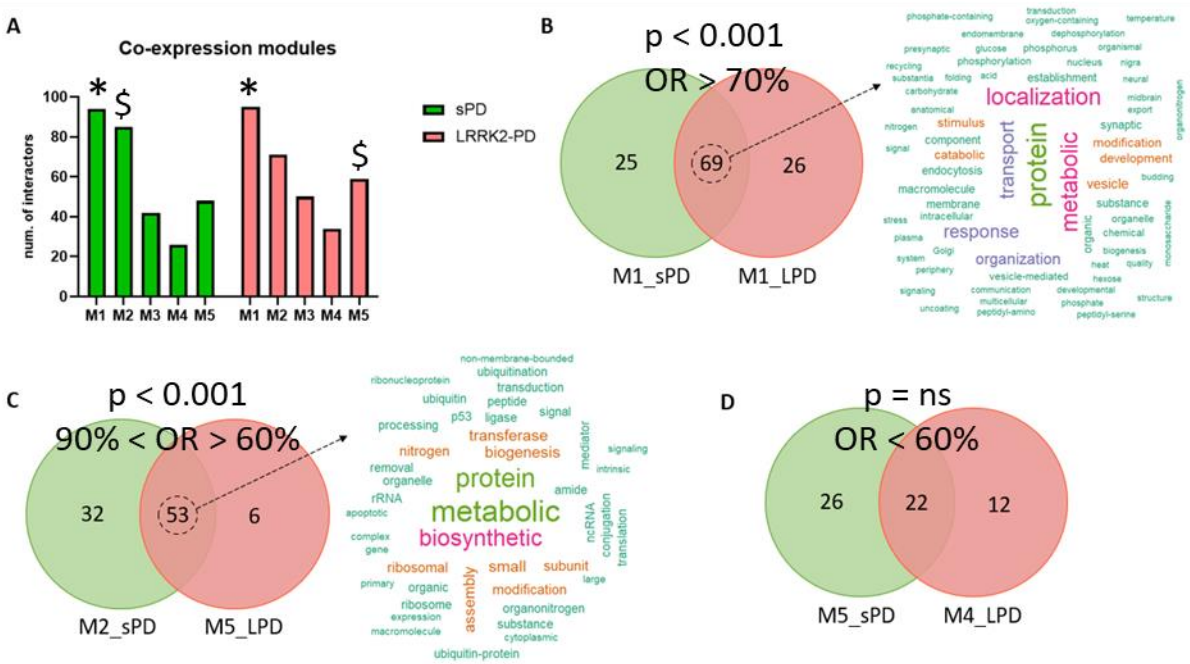

Figure 3. Co-expression modules in LRRK2$_{net}$ A) *The bar graph shows the co-expression modules identified by WGCNA in the sPD and LRRK2-PD cohorts (numbered from 1 to 5). Modules identified with * or $ are statistically similar in node composition.* ***B, C)*** *The Venn graph shows 2 pairs of co-expression modules (M1_sPD vs. M1_LPD and M2_sPD vs. M5_LPD) that significantly overlap ($p < 0.05$ and Overlap Rate (OR) > 60%). The word clouds represent the summary of the functional keywords returned from GO-BP enrichment analysis. The larger the text, the more often it showed in the enrichment results.* ***D)*** *The Venn graph shows the pair of co-expression modules (M5_sPD vs.*

M4_LPD) containing LRRK2 itself, of not the overlap of these modules is not statistically significant, thus these 2 modules are different in terms of node composition.

Identification of topological clusters in the $LRRK2_{net}$ and weighted network analysis

The $LRRK2_{net}$ was QC-ed based on topological features considering that 79 out of 418 interactors (18.9%) showed a degree = 1, i.e., only possessed connection with LRRK2 but not with the other members of the LRRK2 interactome and were thereby discarded for the clustering analysis. In addition, 2 triangle motifs were identified in the $LRRK2_{net}$ (**Figure 1A**). Each triangle motif comprised LRRK2 and 2 other interactors with degree of 2 (interacting between each other but not with the rest of the network). The 4 interactors in these triangle motifs were also excluded from further clustering. Finally, LRRK2 itself was removed from the network, thereby generating the trimmed-$LRRK2_{net}$, containing 338 nodes and 1345 edges.

A total of 14 topological clusters were identified in the trimmed-$LRRK2_{net}$ using the Fast Greedy algorithm based on the measure of edge betweenness (i.e., calculating the number of shortest paths between any pair of nodes in the network that pass-through a given edge). A total of 3 clusters containing less than 5 interactors each were removed, leaving a total of 11 clusters for further analysis (**Table S7**). Each topological cluster was classified using the values previously calculated from DEA and CEA to verify whether the cluster was up/down-regulated (or unaffected) by PD in comparison with controls (sPD or LRRK2-PD vs controls). Specifically, edges were scored into 3 categories: up-regulated, down-regulated or unmodified edge based on changes in the absolute expression levels or co-expression behaviour of the 2 nodes each edge connected. The distribution of the edges across these 3 categories was compared via One Sample Proportion Test to identified clusters significantly altered in expression in sPD or LRRK2-PD in comparison with controls (**Figure 4A, B**). Among the 11 clusters, only cluster A was significantly down-regulated in both sPD and LRRK2-PD vs controls ($p < 0.05$), with 72/115 (62.6%) and 57/115 (49.5%) edges down-regulated, respectively. Of note, the downregulation was a consequence of reduction in node expression in PD vs controls rather than a reduction of the co-expression coefficients (44 edges (61.1%) and 41 edges (71.9%) (**Figure 5A**). GO-BP enrichment analysis returned a total of 42 terms for Cluster A, which related the cluster with functional key words: “biosynthesis”, “metabolic” and “rRNA”, suggesting that sPD and LRRK2-PD potentially contribute to a decreased gene expression and/or ribosomal function generally regulated by this cluster of LRRK2 interactors (**Figure 5A, Table S8**). Cluster H exhibited significant up-regulation in LRRK2-PD only, with 13/21 (76.2%) edges affected by increased expression level of interactors while 3 affected by increased co-expression level between interactors (**Figure 5B**). Of note, up-regulated PRKN expression level contributed to 10/16 altered edges due to its central role in the cluster (degree = 11). Functional enrichment analysis showed that Cluster H was related with functional key words of “mitochondrial”, “localisation”, “response” and “autophagy”, suggesting that during LRRK2-PD progression, regulation of mitochondrial homeostasis as well as autophagy mechanisms are potentially stimulated. (**Figure 5B, Table S8**).

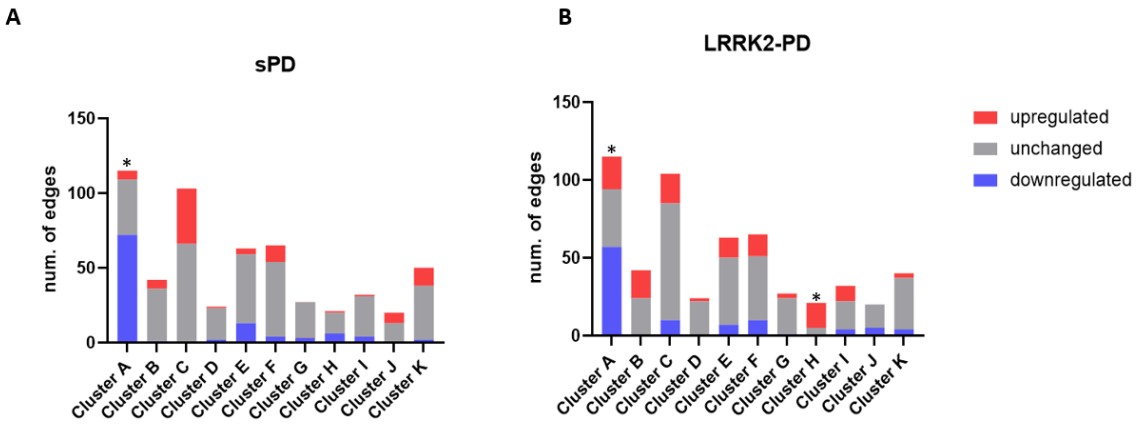

Figure 4. Topological Clustering of the LRRK2$_{net}$ ***A)*** *The bar graph shows the impact of expression behaviour linked with the sPD condition on the edges of each topological cluster. Upregulated edges (in red) were defined as: 1) with ≥ 1 connected interactor exhibiting increased expression level in sPD condition as compared to controls; and/or 2) the 2 connected interactors were positively co-expressed (with Pearson's coefficient > 0.6) in sPD condition but not in controls. Downregulated edges (in blue) were defined in the opposite way: 1) with ≥ 1 connected interactor exhibiting decreased expression level in sPD condition as compared to controls; and/or 2) the 2 connected interactors were positively co-expressed (with Pearson's coefficient > 0.6) in controls but not in sPD. The percentage of upregulated, unchanged and downregulated edges were compared within each cluster via One Sample Proportion test. Only Cluster A was significantly downregulated in sPD (p < 0.001, *).* ***B)*** *The bar graph shows the impact of expression behaviour linked with the LRRK2-PD condition on the edges of each topological cluster. Cluster A was significantly downregulated in LRRK2-PD (p < 0.05, *); while Cluster H was significantly upregulated by LRRK2-PD, (p < 0.001, *) in comparison with controls.*

Finally, the granular differences in cluster A for sPD and LRRK2-PD were considered, and edges were further weighted based on the extent of their up/down-regulation (please refer to material and methods). Edges fell into 7 categories ranging from highly up-regulated to highly down-regulated (**Figure 5C).** Edges in Cluster A presented distinct alteration patterns in the sPD and LRRK2-PD conditions (Chi-square p-value < 0.001), in which more edges experienced moderate downregulation ($S_{(i,j)}$ = -1) in the sPD condition as compared to the LRRK2-PD (N = 28 vs. 14, p = 0.017); while more upregulated edges were found in the LRRK2-PD condition as compared to the sPD (N = 25 vs. 6, p < 0.001), suggesting that although Cluster A presented a similar trend of downregulation overall in comparison with controls (average edge score for cluster A = -2.12 in sPD and -2.23 in LRRK2-PD), the cluster actually exhibited different granular responses and was differently modulated in the 2 types of PD conditions.

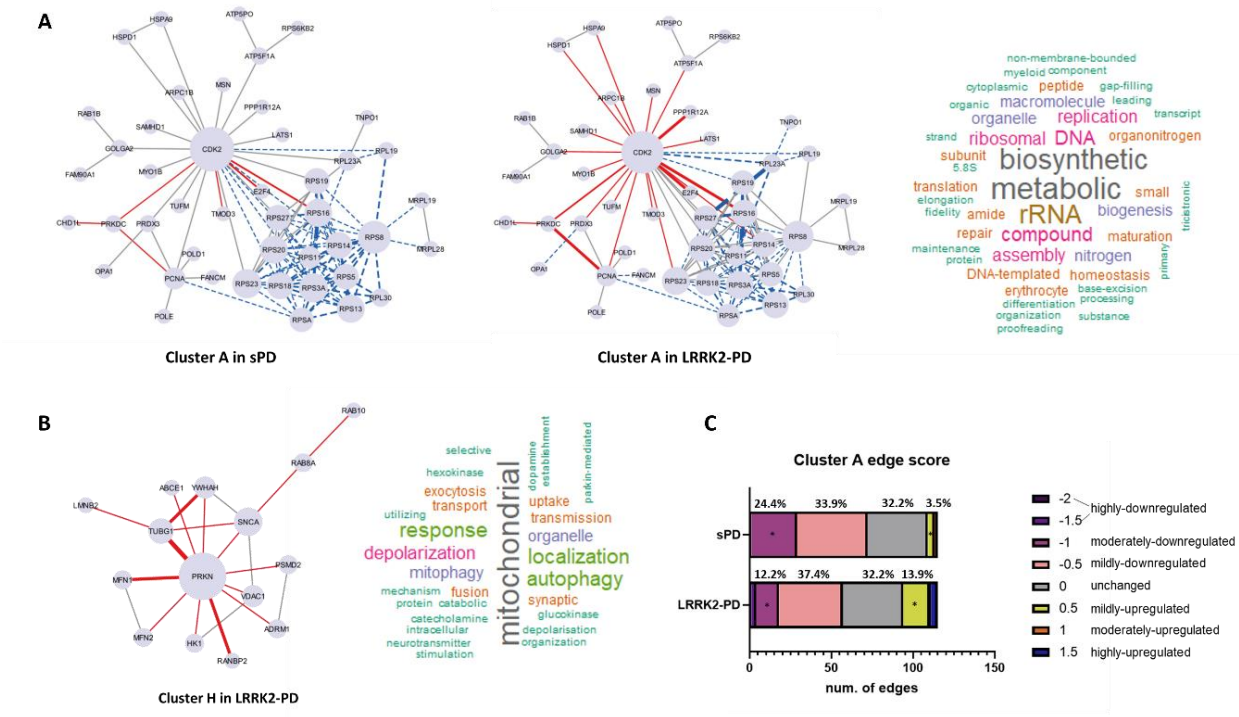

<u>Figure 5. Significantly altered topological clusters in LRRK2$_{net}$</u> ***A)*** *The network graph shows the significant downregulation of Cluster A in sPD and LRRK2-PD, in which LRRK2 interactors are represented as nodes (N = 45) while PPIs are represented as edges (N = 115). Edges are represented with a continuous red line if they are upregulated, with a dotted blue line if they are downregulated. The thickness of the edges is proportional to the calculated S (= edge-score/weight). Word cloud shows the functional keywords returned for Cluster A. The larger the text, the more often it showed in the enrichment results.* ***B)*** *The network graph shows the significant upregulated Cluster H in LRRK2-PD, with interactors represented as nodes (N = 15) and PPIs represented as edges (N = 21). Word cloud shows the functional keywords returned for Cluster H. The larger the text, the more often it showed in the enrichment results.* ***C)*** *The bar graph shows the granular expression alterations of edges in Cluster A in the 2 PD conditions. The overall pattern was compared via Pearson's Chi-square test, giving a p-value < 0.001, suggesting the alterations of Cluster A are significantly different in sPD as compared to LRRK2-PD. The percentage of edges in each score group was compared via One Sample Proportion test. Significant differences were observed in the edge group of "moderately downregulated" and "mildly-upregulated" (p < 0.05, *).*

Discussion

Complex neurodegenerative disorders present with a complicated aetiopathogenesis, triggered by multiple causative events (or risk factors) from the environment and from the genome. An additional layer of complexity is due to the cocktail of risk factors being cohort specific. In PD, for example, most of the patients have a sporadic form of the disease, with no large effect size mutations contributing to it; we generally think these cases are due to a complex set of small effect size genetic risk factors in combination with a triggering environmental exposure. On the other hand, a minority of patients is considered familial with at least one mutation with effect size large enough to drive disease. The sporadic and the genetic forms of PD are, therefore, clearly triggered by different combinations of risk factors. It is legitimate to ask whether, despite the similar clinical presentation and the classification under the same disease name, sporadic and genetic forms might represent a more nuanced spectrum

of disorders. This seemingly philosophical question holds the key to a very practical issue. Sporadic disorders are difficult to be modelled *in vitro*, thus the scientific community relies on genetic models based on the familial forms of the same disease to simulate the disease scenario in a test tube. These experimental models might not be accurate if we are indeed dealing with a spectrum disorder where the same clinical manifestation may be triggered by different molecular scenarios. Similarly, a therapeutic approach targeted to the molecular core of the neurodegeneration developed for the genetic forms of the disease might not be fully effective on the sporadic disease, thus requiring cohort specific interventions.

In this study, we used systems biology to generate a model and investigate the potential molecular differences between sPD and LRRK2-PD, focusing on the transcriptomic expression profile of the LRRK2 protein interactome. We considered, in fact, that the LRRK2 functionality is orchestrated by the protein interactions that interlink LRRK2 with the cell proteome. It is known that LRRK2 interaction behaviour is affected by the presence of mutations (Manzoni et al., 2015); we therefore speculated that the presence of PD causing mutations in LRRK2 (LRRK2-PD) will modify the LRRK2 connectivity and in turn this will trigger expression changes within the LRRK2 interactome. These changes might be specific of the LRRK2-PD scenario since no LRRK2 mutations are present in sPD. However, it is also possible that expression changes of the LRRK2 interactome might happen just as a consequence of PD, in a feedback response to the molecular alterations induced by the disease; in this case these alterations should be evident in both presence (LRRK2-PD) and absence (sPD) of LRRK2 mutations.

When we checked for alterations in expression levels (cases vs controls) for the LRRK2 interactors, 26.5% (100/377) of the LRRK2 interactors presented indeed significant alteration in whole blood mRNA, among which only 17 showed similar trend of alteration (3 up-regulated and 14 down-regulated) between sPD and LRRK2-PD. Functional enrichment of these 17 proteins with similar trend of alteration in both sPD and LRRK2-PD indicated biological processes related to ribosomal activity and protein biosynthesis. It is interesting to note that, among the 100 LRRK2 interactors that were significantly altered in expression levels (all cases vs controls), 23 were ribosomal proteins (RP). These RPs were all down-regulated in the disease scenario: 6 were down-regulated in LRRK2-PD only; 8 were down-regulated in sPD only while 9 were down-regulated in both sPD and LRRK2-PD. This first analysis of the model suggested that, globally, sPD and LRRK2-PD possess distinct molecular signature of expression changes for the LRRK2 interactors. However, a small overlap in expression change does exist between the 2 conditions and this seems associated with those LRRK2 interactors that aid LRRK2 in its functions in the regulation of protein synthesis and ribosomal activity.

We then analysed the co-expression behaviour of the LRRK2 interactome using the classical WGCNA pipeline. We identified 5 co-expression modules in the sPD as well as in the LRRK2-PD $LRRK2_{net}$. We considered the node composition of these 5 modules to verify whether they were consistent between the 2 conditions. Results showed that 2 modules were in fact the same between sPD and LRRK2-PD while 3 were statistically different. The 2 modules shared between sPD and LRRK2-PD again were composed of proteins relevant for processes of protein biosynthesis, protein transport, ribosomal and in general metabolic activity. Of interest, 21 out of the 23 significantly altered RB present in the LRRK2 interactome (91.3%) presented high co-expression between each other and were allocated into the same WGCNA module in both sPD and LRRK2-PD, again confirming these processes and players might be consistently altered in the 2 disease scenarios.

The topological clustering algorithm identified 11 clusters in the $LRRK2_{net}$, these are portions of the network that are more connected within each other than the average connection of the entire network. The majority of the RP were, as expected, contained within one cluster and interestingly this cluster was the only one whose global change in expression and co-expression was overall statistically

significant (cases vs controls) in both sPD and LRRK2-PD. In particular this cluster was significantly downregulated, potentially suggesting that the functionality of RPs and ribosomal, protein biosynthetic processes are universally reduced during PD. This finding is in accordance with several previous functional studies that found similar down-regulation in RPs in whole blood and substantia nigra in sPD patients as well as LRRK2-G2019S PD patients as compared to controls (Scherzer *et al.*, 2007; Garcia-Esparcia *et al.*, 2015; Flinkman *et al.*, 2023; Jang *et al.*, 2023). The other network cluster that was significantly modified considering its expression behaviour in cases vs controls contained 15 LRRK2 interactors with general up-regulation; however, this cluster was only significantly modified in LRRK2-PD, not in sPD while compared to control. The function of this cluster was associated with Parkin-dependent mitophagy, and indeed PRKN/Parkin was at the centre of the cluster connectivity suggesting an interlink between of the effect of LRRK2 mutation (G2019S and/or R1441C) and the well-established mitophagy alterations in PD. Multiple lines of evidence have indicated that increased LRRK2 kinase activity negatively affects Parkin-dependent mitophagy. For example, structural biology study have found that overexpression of LRRK2 and LRRK2-G2019S interrupts the PPI between Parkin and other key proteins essential for mitophagy on the outer mitochondrial membrane, and thereby interferes with the recruitment of Parkin with disruption of mitophagy (Bonello et al., 2019; Lin et al., 2021) This may explain the up-regulated PRKN/Parkin expression level cluster as observed in our study – as a compensation for reduced interactable Parkin at the mitochondria. Also, the increased co-expression between PRKN/Parkin and MFN1, TUBG1 as well as RANBP2 may serve as compensation mechanism for the altered mitochondrial fusion/fission dynamics in the presence of LRRK2-G2019S, which have been reported in several studies (Bradshaw et al., 2021; Gegg et al., 2010). There are a few limitations in this study: 1) the sample size of the cohorts are relatively small, especially for the LRRK2-PD cohort. Larger sample size would improve statistical power and thereby give more robust results; 2) PD cases recruited by PPMI were at the early stages of the disease and the whole blood mRNA sequencing was run at the first visit. Therefore, the alterations of some LRRK2 interactors could be too subtle to be detected by DEA or WGCNA; 3) the LRRK2-PD cohort includes both G2019S and R1441C/G mutations and thereby introduce subtle bias due to genetic variation.

In conclusion, our study suggests that although sPD and LRRK2-PD clearly share aspects of the PD pathology and PD clinical presentation, the molecular pathways at the basis of the 2 conditions might be slightly different. There are shared changes of the LRRK2 interactome that can be appreciated at the transcriptome level in both the 2 conditions, and these are mainly associated with alterations of ribosomal proteins and proteins whose function is important for protein biosynthesis. However, there are also large differences between the 2 conditions suggested by the unique transcriptomics signatures. This conclusion suggests that LRRK2-PD and sPD should not be treated as the same conditions, prompts the request for experimental models to be generated as specific for the condition under analysis and confirms the requirement for patient stratification.

Data Availability

Data used in the preparation of this article were obtained [on 24th January 2023] from the Parkinson's Progression Markers Initiative (PPMI) database (www.ppmi-info.org/access-data-specimens/download-data), RRID:SCR_006431. For up-to-date information on the study, visit www.ppmi-info.org.

Acknowledgments

CM and VEP received funding from the MJFF (grant number MJFF-021335). PAL and CM acknowledge funding from the Biomarkers Across Neurodegenerative Diseases Grant Program 2019, BAND3 (Michael J. Fox Foundation, Alzheimer's Association, Alzheimer's Research UK, and the Weston Brain

Institute [grant number 18063]). Funding: PPMI – a public-private partnership – is funded by the Michael J. Fox Foundation for Parkinson's Research and funding partners, including 4D Pharma, Abbvie, AcureX, Allergan, Amathus Therapeutics, Aligning Science Across Parkinson's, AskBio, Avid Radiopharmaceuticals, BIAL, Biogen, Biohaven, BioLegend, BlueRock Therapeutics, Bristol-Myers Squibb, Calico Labs, Celgene, Cerevel Therapeutics, Coave Therapeutics, DaCapo Brainscience, Denali, Edmond J. Safra Foundation, Eli Lilly, Gain Therapeutics, GE HealthCare, Genentech, GSK, Golub Capital, Handl Therapeutics, Insitro, Janssen Neuroscience, Lundbeck, Merck, Meso Scale Discovery, Mission Therapeutics, Neurocrine Biosciences, Pfizer, Piramal, Prevail Therapeutics, Roche, Sanofi, Servier, Sun Pharma Advanced Research Company, Takeda, Teva, UCB, Vanqua Bio, Verily, Voyager Therapeutics, the Weston Family Foundation and Yumanity Therapeutics.

Reference

Alanis-Lobato, G., Andrade-Navarro, M. A., & Schaefer, M. H. (2017). HIPPIE v2.0: Enhancing meaningfulness and reliability of protein-protein interaction networks. *Nucleic Acids Research*, *45*(D1), D408–D414. https://doi.org/10.1093/nar/gkw985

Albanese, F., Novello, S., & Morari, M. (2019). Autophagy and LRRK2 in the Aging Brain. *Frontiers in Neuroscience*, *13*, 1352. https://doi.org/10.3389/FNINS.2019.01352/BIBTEX

Alcalay, R. N., Mejia-Santana, H., Mirelman, A., Saunders-Pullman, R., Raymond, D., Palmese, C., Caccappolo, E., Ozelius, L., Orr-Urtreger, A., Clark, L., Giladi, N., Bressman, S., Marder, K., Tang, M. X., Santana, H. M., Roos, E., Orbe-Reilly, M., Fahn, S., Cote, L., … Ortega, R. (2015). Neuropsychological performance in LRRK2 G2019S carriers with Parkinson's disease. *Parkinsonism & Related Disorders*, *21*(2), 106–110. https://doi.org/10.1016/J.PARKRELDIS.2014.09.033

Batzu, L., Urso, D., Grothe, M. J., Veréb, D., Chaudhuri, K. R., & Pereira, J. B. (2023). Increased basal forebrain volumes could prevent cognitive decline in LRRK2 Parkinson's disease. *Neurobiology of Disease*, *183*. https://doi.org/10.1016/J.NBD.2023.106182

Berwick, D. C., Heaton, G. R., Azeggagh, S., & Harvey, K. (2019). LRRK2 Biology from structure to dysfunction: Research progresses, but the themes remain the same. *Molecular Neurodegeneration*, *14*(1), 1–22. https://doi.org/10.1186/s13024-019-0344-2

Bonello, F., Hassoun, S. M., Mouton-Liger, F., Shin, Y. S., Muscat, A., Tesson, C., Lesage, S., Beart, P. M., Brice, A., Krupp, J., Corvol, J. C., & Corti, O. (2019). LRRK2 impairs PINK1/Parkin-dependent mitophagy via its kinase activity: pathologic insights into Parkinson's disease. *Human Molecular Genetics*, *28*(10), 1645–1660. https://doi.org/10.1093/HMG/DDZ004

Bradshaw, A. V., Campbell, P., Schapira, A. H. V., Morris, H. R., & Taanman, J. W. (2021). The PINK1-Parkin mitophagy signalling pathway is not functional in peripheral blood mononuclear cells. *PloS One*, *16*(11). https://doi.org/10.1371/JOURNAL.PONE.0259903

Bras, J. M., Guerreiro, R. J., Ribeiro, M. H., Januario, C., Morgadinho, A., Oliveira, C. R., Cunha, L., Hardy, J., & Singleton, A. (2005). G2019S dardarin substitution is a common cause of Parkinson's disease in a Portuguese cohort. *Movement Disorders : Official Journal of the Movement Disorder Society*, *20*(12), 1653–1655. https://doi.org/10.1002/mds.20682

Chen, Z., Cao, Z., Zhang, W., Gu, M., Zhou, Z. D., Li, B., Li, J., Tan, E. K., & Zeng, L. (2017). LRRK2 interacts with ATM and regulates Mdm2–p53 cell proliferation axis in response to genotoxic stress. *Human Molecular Genetics*, *26*(22), 4494–4505. https://doi.org/10.1093/HMG/DDX337

Cook, D. A., Kannarkat, G. T., Cintron, A. F., Butkovich, L. M., Fraser, K. B., Chang, J., Grigoryan, N., Factor, S. A., West, A. B., Boss, J. M., & Tansey, M. G. (2017). LRRK2 levels in immune cells are increased in Parkinson's disease. *NPJ Parkinson's Disease*, *3*(1). https://doi.org/10.1038/S41531-017-0010-8

Dauer, W., & Ho, C. C. Y. (2010). The biology and pathology of the familial Parkinson's disease protein LRRK2. *Movement Disorders : Official Journal of the Movement Disorder Society*, *25 Suppl 1*(SUPPL. 1). https://doi.org/10.1002/MDS.22717

Di Maio, R., Hoffman, E. K., Rocha, E. M., Keeney, M. T., Sanders, L. H., De Miranda, B. R., Zharikov, A., Van Laar, A., Stepan, A. F., Lanz, T. A., Kofler, J. K., Burton, E. A., Alessi, D. R., Hastings, T. G., & Timothy Greenamyre, J. (2018). LRRK2 activation in idiopathic Parkinson's disease. *Science Translational Medicine*, *10*(451). https://doi.org/10.1126/SCITRANSLMED.AAR5429

Esteves, A. R., Swerdlow, R. H., & Cardoso, S. M. (2014). LRRK2, a puzzling protein: insights into Parkinson's disease pathogenesis. *Experimental Neurology*, *261*, 206–216. https://doi.org/10.1016/J.EXPNEUROL.2014.05.025

Garrido, A., Fairfoul, G., Tolosa, E. S., Martí, M. J., & Green, A. (2019). α-synuclein RT-QuIC in cerebrospinal fluid of LRRK2-linked Parkinson's disease. *Annals of Clinical and Translational Neurology*, *6*(6), 1024–1032. https://doi.org/10.1002/ACN3.772

Gegg, M. E., Cooper, J. M., Chau, K. Y., Rojo, M., Schapira, A. H. V., & Taanman, J. W. (2010). Mitofusin 1 and mitofusin 2 are ubiquitinated in a PINK1/parkin-dependent manner upon induction of mitophagy. *Human Molecular Genetics*, *19*(24), 4861. https://doi.org/10.1093/HMG/DDQ419

Giesert, F., Glasl, L., Zimprich, A., Ernst, L., Piccoli, G., Stautner, C., Zerle, J., Hölter, S. M., Vogt Weisenhorn, D. M., & Wurst, W. (2017). The pathogenic LRRK2 R1441C mutation induces specific deficits modeling the prodromal phase of Parkinson's disease in the mouse. *Neurobiology of Disease*, *105*, 179–193. https://doi.org/10.1016/j.nbd.2017.05.013

Greggio, E., Zambrano, I., Kaganovich, A., Beilina, A., Taymans, J. M., Daniëls, V., Lewis, P., Jain, S., Ding, J., Syed, A., Thomas, K. J., Baekelandt, V., & Cookson, M. R. (2008). The Parkinson disease-associated leucine-rich repeat kinase 2 (LRRK2) is a dimer that undergoes intramolecular autophosphorylation. *Journal of Biological Chemistry*, *283*(24), 16906–16914. https://doi.org/10.1074/jbc.M708718200

Haugarvoll, K., Rademakers, R., Kachergus, J. M., Nuytemans, K., Ross, O. A., Gibson, J. M., Tan, E. K., Gaig, C., Tolosa, E., Goldwurm, S., Guidi, M., Riboldazzi, G., Brown, L., Walter, U., Benecke, R., Berg, D., Gasser, T., Theuns, J., Pals, P., … Wszolek, Z. K. (2008). Lrrk2 R1441C parkinsonism is clinically similar to sporadic Parkinson disease. *Neurology*, *70*(16 Part 2), 1456–1460. https://doi.org/10.1212/01.WNL.0000304044.22253.03

Healy, D. G., Wood, N. W., & Schapira, A. H. V. (2008). Test for LRRK2 mutations in patients with Parkinson's disease. *Practical Neurology*, *8*(6), 381–385. https://doi.org/10.1136/JNNP.2008.162420

Henry, A. G., Aghamohammadzadeh, S., Samaroo, H., Chen, Y., Mou, K., Needle, E., & Hirst, W. D. (2015). Pathogenic LRRK2 mutations, through increased kinase activity, produce enlarged lysosomes with reduced degradative capacity and increase ATP13A2 expression. *Human Molecular Genetics*, *24*(21), 6013–6028. https://doi.org/10.1093/hmg/ddv314

Hsu, C. H., Chan, D., & Wolozin, B. (2010). LRRK2 and the Stress Response: Interaction with MKKs and JNK-Interacting Proteins. *Neuro-Degenerative Diseases*, *7*(1–3), 68. https://doi.org/10.1159/000285509

Hu, Y., Vinayagam, A., Nand, A., Comjean, A., Chung, V., Hao, T., Mohr, S. E., & Perrimon, N. (2018). Molecular Interaction Search Tool (MIST): An integrated resource for mining gene and protein interaction data. *Nucleic Acids Research*, *46*(D1), D567–D574. https://doi.org/10.1093/nar/gkx1116

Kluss, J. H., Mamais, A., & Cookson, M. R. (2019). LRRK2 links genetic and sporadic Parkinson's disease. *Biochemical Society Transactions*, *47*(2), 651. https://doi.org/10.1042/BST20180462

Langfelder, P., & Horvath, S. (2008). WGCNA: An R package for weighted correlation network analysis. *BMC Bioinformatics*, *9*. https://doi.org/10.1186/1471-2105-9-559

Lesage, S., Dürr, A., Tazir, M., Lohmann, E., Leutenegger, A.-L., Janin, S., Pollak, P., & Brice, A. (2006). LRRK2 G2019S as a cause of Parkinson's disease in North African Arabs. In *The New England journal of medicine* (Vol. 354, Issue 4, pp. 422–423). https://doi.org/10.1056/NEJMc055540

Lin, J., Zheng, X., Zhang, Z., Zhuge, J., Shao, Z., Huang, C., Jin, J., Chen, X., Chen, Y., Wu, Y., Tian, N., Sun, L., Gao, W., Zhou, Y., Wang, X., & Zhang, X. (2021). Inhibition of LRRK2 restores parkin-mediated mitophagy and attenuates intervertebral disc degeneration. *Osteoarthritis and Cartilage*, *29*(4), 579–591. https://doi.org/10.1016/J.JOCA.2021.01.002

Manzoni, C., Denny, P., Lovering, R. C., & Lewis, P. A. (2015). Computational analysis of the LRRK2 interactome. *PeerJ*, *2015*(2). https://doi.org/10.7717/peerj.778

Nalls, M. A., Blauwendraat, C., Vallerga, C. L., Heilbron, K., Bandres-Ciga, S., Chang, D., Tan, M., Kia, D. A., Noyce, A. J., Xue, A., Bras, J., Young, E., von Coelln, R., Simón-Sánchez, J., Schulte, C., Sharma, M., Krohn, L., Pihlstrøm, L., Siitonen, A., … Zhang, F. (2019). Identification of novel risk loci, causal insights, and heritable risk for Parkinson's disease: a meta-analysis of genome-wide association studies. *The Lancet. Neurology*, *18*(12), 1091–1102. https://doi.org/10.1016/S1474-4422(19)30320-5

Ozelius, L. J., Senthil, G., Saunders-Pullman, R., Ohmann, E., Deligtisch, A., Tagliati, M., Hunt, A. L., Klein, C., Henick, B., Hailpern, S. M., Lipton, R. B., Soto-Valencia, J., Risch, N., & Bressman, S. B. (2006). LRRK2 G2019S as a cause of Parkinson's disease in Ashkenazi Jews. In *The New England journal of medicine* (Vol. 354, Issue 4, pp. 424–425). https://doi.org/10.1056/NEJMc055509

Paisán-Ruiz, C., Lewis, P. A., & Singleton, A. B. (2013). LRRK2: cause, risk, and mechanism. *Journal of Parkinson's Disease*, *3*(2), 85–103. https://doi.org/10.3233/JPD-130192

Raudvere, U., Kolberg, L., Kuzmin, I., Arak, T., Adler, P., Peterson, H., & Vilo, J. (2019). G:Profiler: A web server for functional enrichment analysis and conversions of gene lists (2019 update). *Nucleic Acids Research*, *47*(W1), W191–W198. https://doi.org/10.1093/nar/gkz369

Rivero-Ríos, P., Romo-Lozano, M., Fasiczka, R., Naaldijk, Y., & Hilfiker, S. (2020). LRRK2-Related Parkinson's Disease Due to Altered Endolysosomal Biology With Variable Lewy Body Pathology: A Hypothesis. *Frontiers in Neuroscience*, *14*, 556. https://doi.org/10.3389/FNINS.2020.00556/BIBTEX

Sanna, G., Del Giudice, M. G., Crosio, C., & Iaccarino, C. (2012). LRRK2 and vesicle trafficking. *Biochemical Society Transactions*, *40*(5), 1117–1122. https://doi.org/10.1042/BST20120117

Shannon, P., Markiel, A., Ozier, O., Baliga, N. S., Wang, J. T., Ramage, D., Amin, N., Schwikowski, B., & Ideker, T. (2003a). Cytoscape: a software environment for integrated models of biomolecular interaction networks. *Genome Research*, *13*(11), 2498–2504. https://doi.org/10.1101/gr.1239303

Shannon, P., Markiel, A., Ozier, O., Baliga, N. S., Wang, J. T., Ramage, D., Amin, N., Schwikowski, B., & Ideker, T. (2003b). Cytoscape: A software Environment for integrated models of biomolecular interaction networks. *Genome Research*, *13*(11), 2498–2504. https://doi.org/10.1101/gr.1239303

Srivatsal, S., Cholerton, B., Leverenz, J. B., Wszolek, Z. K., Uitti, R. J., Dickson, D. W., Weintraub, D., Trojanowski, J. Q., Van Deerlin, V. M., Quinn, J. F., Chung, K. A., Peterson, A. L., Factor, S. A., Wood-Siverio, C., Goldman, J. G., Stebbins, G. T., Bernard, B., Ritz, B., Rausch, R., … Zabetian, C. P. (2015). Cognitive profile of LRRK2-related Parkinson's disease. *Movement Disorders : Official Journal of the Movement Disorder Society*, *30*(5), 728–733. https://doi.org/10.1002/MDS.26161

Tolosa, E., Vila, M., Klein, C., & Rascol, O. (2020). LRRK2 in Parkinson disease: challenges of clinical trials. In *Nature Reviews Neurology* (Vol. 16, Issue 2, pp. 97–107). Nature Research. https://doi.org/10.1038/s41582-019-0301-2

Tomkins, J. E., Ferrari, R., Vavouraki, N., Hardy, J., Hardy, J., Hardy, J., Hardy, J., Hardy, J., Lovering, R. C., Lewis, P. A., Lewis, P. A., Lewis, P. A., McGuffin, L. J., Manzoni, C., & Manzoni, C. (2020). PINOT: An intuitive resource for integrating protein-protein interactions. *Cell Communication and Signaling*, *18*(1). https://doi.org/10.1186/s12964-020-00554-5

Zhao, Y., Vavouraki, N., Lovering, R. C., Escott-Price, V., Harvey, K., Lewis, P. A., & Manzoni, C. (2023). Tissue specific LRRK2 interactomes reveal a distinct striatal functional unit. *PLoS Computfile:///Users/Zhaoyibo/Downloads/PIIS0021925820714961.Pdfational Biology*, *19*(1), 1–23. https://doi.org/10.1371/journal.pcbi.1010847